

Numerical Simulation of the One-dimensional Quantum Harmonic Oscillator

RODRIGO PEREIRA SILVA

Instituto de Física da Universidade de São Paulo
São Paulo – SP

Abstract

The importance of Quantum Mechanics for science and technology in the last century is undeniable. One of the most important results from the quantum mechanics formalism are those of the harmonic oscillators, since they represent a broad class of phenomena and the possibility of approximating much more complex systems in a treatable fashion. This study aims to simulate numerically the dynamics of a one-dimensional harmonic oscillator with initial states being eigen-states of the Hamiltonian, eigen-states with a spatial phase, and linear combination (LC) of eigen-states. The numerical method used to simulate these dynamics was Runge-Kutta's second order approximation to solve the time-dependent Schrödinger's equation, with the well known harmonic potential. Ehrenfest's theorem is also tested, as well as Heisenberg's uncertainty principle, both of them showing good agreement with theoretical developments. A case where an initial spatial phase term is added to the initial wave function, resulting in a change of the expected values of position and momentum, which yields in a probability distribution function (PDF) that maintains its shape, although it oscillates through time. Another case where the initial state is a LC of eigen-states show that the PDF is now time-dependent. An examination of the normalization of the PDF for different wave functions show that it fails at higher vibration modes, indicating that the dynamics of higher frequencies of oscillation are better captured by further time discretizations. Animations showing many of the examined effects were produced and can be accessed at [Notion](#).

I. INTRODUCTION

We must be clear that when it comes to atoms, language can be used only as in poetry.

Niels Bohr

Quantum Mechanics is the background over which one of the biggest scientific revolutions of humanity has developed, and later would make it possible for great technological accomplishments, as well as a renewal of our way of thinking about science and to interpret reality as a whole. The first half of the XX century was bubbling with new ideas, experiments, and break of expectations that used to be marked in stone. The little is now different from the big: it is strange to us. The Heisenberg uncertainty principle shows that now there are incompatible dynamical variables that cannot be measured simultaneously; now probability is not classical anymore, but is rather a fundamental concept of nature itself. The observables, physical quantities of interest that we used to be measured and treated like common numbers that follow common commutation rules are now replaced by operators: agents that do not commute trivially. Schrödinger's equation, similarly to Newton's second law, is responsible to

show how a system evolves with time, given some dynamics and the proper initial conditions. This equation requires two things only: the state vector is at all times normalized, and the time evolution is linear. The former provides a probabilistic way of seeing the vector state and its results upon measurement, and the latter demands that the time evolution, besides being linear, is also unitary [1].

The above considerations lead to a general format to Schrödinger's equation, given by¹

$$\frac{\partial}{\partial t} |\psi(t)\rangle = -i\hat{H}(t) |\psi(t)\rangle, \quad (1)$$

where $|\psi(t)\rangle$ is the state vector, \hat{H} is the Hamiltonian of the system, which dictates the dynamics in which the experiment will evolve upon. It is important to notice that Eq. (1) only gives a format for the evolution of a physical system. Identification of the operator \hat{H} as the Hamiltonian and its components is usually done by mathematical and experimental arguments [2]. The Hamiltonian operator is inspired by its classical counterpart, given by

$$\hat{H} = \frac{\hat{p}^2}{2m} + V(\hat{x}), \quad (2)$$

where \hat{p} and \hat{x} are operators of linear momentum and position,

¹To take it out of the way: during the whole course of this study, the choice of units is such that $\hbar = m = 1$.

respectively, and which obey the canonical commutation rule

$$[\hat{x}, \hat{p}] = i. \quad (3)$$

All the formalism of wave mechanics, with the wave function and the known momentum and position operators can be re-obtained via projection of the state vector on the basis of configurations of the system, that is, $\langle x|\psi(t)\rangle = \psi(x, t)$. In this basis, Schrödinger's equation takes the form

$$-i\frac{\partial}{\partial t}\psi(x, t) = \left[\frac{1}{2}\frac{\partial^2}{\partial x^2} - V(x, t)\right]\psi(x, t). \quad (4)$$

Since the aim of this study is the harmonic oscillator, we shall refer to the potential as time-independent, that is, $V(x, t) = V(x)$. Then, supposing $\psi(x, t)$ is separable in a spatial and a temporal part, we can write it as

$$\psi(x, t) = \phi(x)g(t). \quad (5)$$

Plugging these back into Eq. (4) we get a system of uncoupled equations

$$-\frac{1}{2}\frac{d^2}{dx^2}\phi(x) + V(x)\phi(x) = E\phi(x), \quad (6a)$$

$$i\frac{d}{dt}g(t) = Eg(t), \quad (6b)$$

where E is the uncoupling constant, which will be identified as the energy of the system. The first of the above equations is called time independent Schrödinger equation, whose solution depends on the functional form of the potential. The second one is solvable without knowing the potential, and its solution is

$$g(t) = e^{-iEt}, \quad (7)$$

where the constant that should be multiplying the exponential will be latter absorbed by the spatial solution, so it was omitted here. Then, the full solution for Schrödinger equation is given by

$$\psi(x, t) = \phi(x)e^{-iEt}. \quad (8)$$

This result alone gives some important insight on the probability density function $P(x, t)$, since

$$\begin{aligned} P(x, t) &= |\langle x|\psi(t)\rangle|^2 \\ &= \psi^*(x, t)\psi(x, t)e^{iEt}e^{-iEt} \\ &= |\phi(x)|^2 = P(x). \end{aligned} \quad (9)$$

This result shows that the time-dependent part of the solution does not affect the probability density associated with the wave equation. This characteristic only arises in systems that are subject to time-independent Hamiltonians—which is when separation from Eq. (5) is possible. States whose expected values of observables, as well as the associated PDFs are time-independent are called *stationary states*.

I. Quantum Harmonic Oscillator

The harmonic oscillator is, without any question, one of the most important systems in Physics. From classical to quantum, the versatility of the harmonic oscillator model arises from the fact that any system subject to a well behaved potential $V(x)$ that has a minimum at some point x_0 can have its dynamics approximated, at the neighborhood of this point, by a harmonic oscillator. Inspired by its classical counterpart, the potential of the quantum harmonic oscillator is given by

$$V(\hat{x}) = \frac{1}{2}\omega^2\hat{x}^2, \quad (10)$$

where the classical position x is now replaced by the position operator \hat{x} . Plugging this potential onto Eq. (6a) we get

$$\left(\frac{1}{2}\frac{d^2}{dx^2} - \frac{1}{2}\omega^2x^2\right)\phi(x) = E\phi(x). \quad (11)$$

The details of the solution for the above time-independent equation are not relevant in the current discussion and are discussed in detail in the literature [3, 4, 5], therefore it will suffice to show the result, according to [5]:

$$\phi_n(x) = \frac{1}{\sqrt{2^n n!}}\left(\frac{\omega}{\pi}\right)^{1/4} e^{-\omega x^2/2} H_n\left(\sqrt{\omega}x\right), \quad n = 0, 1, 2, \dots \quad (12)$$

where $H_n(x)$ are the Hermite polynomials of order n , with argument x . These polynomials are given by [3]

$$H_n(z) = (-1)^n e^{z^2} \frac{d^n}{dz^n} e^{-z^2}. \quad (13)$$

Since the harmonic oscillator has a Hamiltonian that does not depend explicitly in time, the time-dependent part of the solution is trivial and is given by Eq. (7), and plugging it together with the spatial solution yields the general solution

$$\psi_n(x, t) = \phi_n(x)e^{-iE_n t}, \quad (14)$$

which is a stationary state and constitute a standing wave inside the limits allowed by the potential.

The term E_n appearing in the solutions above account for the energy of each mode, where n denotes the index of the mode. These energies are given by [6]

$$E_n = \omega\left(n + \frac{1}{2}\right). \quad (15)$$

The first thing to notice is that the ground state energy E_0 is not zero: it is $\omega/2$, which means that at the lowest bound, the quantum harmonic oscillator still has some energy associated with it, so we are still not able to measure its position and momentum at the same time—if the particle has *no* energy whatsoever, it

would be trivial to find x and p . This lowest energy is called *point zero energy* [5].² Another aspect of this formulation that is noteworthy is that, like the eigen-states, the eigen-energies associated with them are also quantized, and unlike Bohr's Hydrogen atom [3] or the particle trapped in the infinite well [8], the energy difference between energy levels is constant, and given by ω .

The family of solutions found $\{\phi_n\}$ form a complete set, which means that any initial state $\varphi(x, 0)$ can be decomposed as

$$\varphi(x, 0) = \sum_{n=0}^{\infty} c_n(0) \phi_n(x), \quad (16)$$

where the c_n 's are the projection of the initial state in the basis formed by the eigen-states, that is,

$$c_n(0) = \langle \phi_n | \varphi(0) \rangle = \int_{-\infty}^{+\infty} \phi_n^*(x) \varphi(x, 0) dx. \quad (17)$$

The time evolution of the system is given by the imaginary exponential term, thus we can write the state $\varphi(x, t)$ at any time t as [9]

$$\begin{aligned} \varphi(x, t) &= \sum_n c_n(0) e^{-iE_n t} \phi_n(x) \\ &= \sum_n c_n(0) e^{-i(n+\frac{1}{2})\omega t} \phi_n(x) \\ &= e^{-i\omega t/2} \sum_n c_n(0) e^{-in\omega t} \phi_n(x) \end{aligned} \quad (18)$$

This generic state generally does not result in a stationary state, that is, its probability density function is time-dependent [3]. For further investigation of such states, see [V](#).

One last thing to point out is the uncertainty relation between momentum and position in the context of the quantum harmonic oscillator. Generally, the uncertainty reads [10]

$$\sigma_x \sigma_p \geq \frac{1}{2}, \quad (19)$$

where σ_x and σ_p are the standard deviations of the position and momentum operators, respectively. In the context of the harmonic oscillator, we have [4]

$$\sigma_x \sigma_p = n + \frac{1}{2}, \quad (20)$$

which indicates compatibility with the foreseen uncertainty. A lower bound is obtained by ground state ψ_0 , given by a Gaussian curve if we look at Eq. (12).

²This feature starts to explain some interesting phenomena, as to why we cannot reach absolute zero temperature; and some more complex things as the spontaneous creation and annihilation of virtual particles that eventually give rise to the Casimir effect [7].

³Another argument to prove this without the need of creation and annihilation operators is by checking the parity of Hermite polynomials: they are odd for n odd and even for n even. Computing the expected value of both \hat{x} and \hat{p} operators eventually falls into integrating an odd function over a symmetrical interval (from $-\infty$ to ∞), so the result is always zero.

II. Ehrenfest's Theorem

The mean value of an observable $\langle \hat{A} \rangle$ is given by [4]

$$\langle \hat{A} \rangle = \langle \psi(t) | \hat{A} | \psi(t) \rangle, \quad (21)$$

where $|\psi(t)\rangle$ is the state vector of the system where we make our measurements. By differentiation of both sides of the above equation we get to

$$\frac{d}{dt} \langle \hat{A} \rangle = -i \langle [\hat{A}, \hat{H}] \rangle + \left\langle \frac{\partial \hat{A}}{\partial t} \right\rangle. \quad (22)$$

Ehrenfest's theorem is obtained by the direct application of this formula to the observables \hat{x} and \hat{p} . These are written as

$$\frac{d}{dt} \langle \hat{x} \rangle = -i \langle [\hat{x}, \hat{H}] \rangle = -i \left\langle \left[\hat{x}, \frac{\hat{p}^2}{2} \right] \right\rangle, \quad (23a)$$

$$\frac{d}{dt} \langle \hat{p} \rangle = -i \langle [\hat{p}, \hat{H}] \rangle = -i \langle [\hat{p}, V(\hat{x})] \rangle. \quad (23b)$$

Replacing the potential in Eq. (23b) for the harmonic oscillator potential and using the canonical commutation relation in Eq. (3), we get

$$\frac{d}{dt} \langle \hat{x} \rangle = \langle \hat{p} \rangle, \quad (24a)$$

$$\frac{d}{dt} \langle \hat{p} \rangle = -\omega^2 \langle \hat{x} \rangle. \quad (24b)$$

The above is a coupled system of differential equations with the expectation values as variables. Integration of these equations yield [4]

$$\langle \hat{x} \rangle_t = \langle \hat{x} \rangle_0 \cos(\omega t) + \frac{1}{\omega} \langle \hat{p} \rangle_0 \sin(\omega t), \quad (25a)$$

$$\langle \hat{p} \rangle_t = \langle \hat{p} \rangle_0 \cos(\omega t) - \omega \langle \hat{x} \rangle_0 \sin(\omega t). \quad (25b)$$

This result is somewhat expected: the mean values of the operators of momentum and position are, themselves, harmonic oscillators. This relates closely with classical mechanics, since the position and momentum—not operators!—are harmonic oscillators, differing only from a phase.

Although this analysis at first sight resembles a lot a classical harmonic oscillator, through the algebraic approach to the quantum harmonic oscillator with the aid of creation and annihilation operators—which is thoroughly covered in [4] and will be not explained here—it is straightforward to show that, for all of the eigen-states of the Hamiltonian given by Eq. (12), the expected values of the position and momentum operators are zero³, so Eqs. (25) are only non-trivial for initial states different from these. Therefore, to explore this property in a not-so-boring system, we will use an initial state changed a bit by a spatial phase that translates into a boost of momentum (see Sec. IV).

III. Classical and quantum oscillator PDFs

The very format of the potential in the quantum harmonic oscillator is given by its classical counterpart; so the comparison between both is inevitable. The probability density function of the classical oscillator P_{cl} is given by [10]

$$P_{cl}(x) = \frac{1}{\pi} \frac{1}{\sqrt{L^2 - x^2}}, \quad (26)$$

where L is the amplitude of the oscillator. It is known that the position and momentum in the classical harmonic oscillator are deterministic, so at first sight the attribution of a probability density function to this system seems nonsense. However, just for a second imagine that we have to point the position of the oscillator with our eyes shut, so the above PDF is the chance of us getting the right result. The probability is bigger in the extremes—where the oscillator spends most of its time at, because it has minimum velocity—and the shortest in the middle, where the velocity is the biggest. A representation of such distribution is shown in Fig. 1.

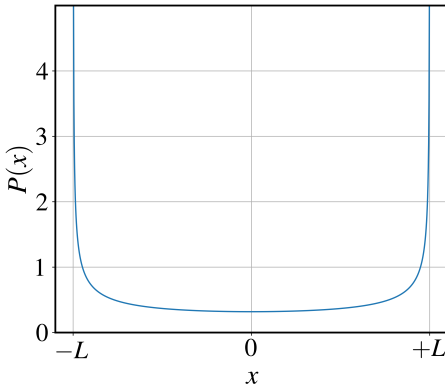


Figure 1: Probability density function for the classical harmonic oscillator. We can see that the probability density is bigger at the maximum length of the oscillation and shorter at the center.

Further analysis will put the probability distributions of the quantum and classical oscillators side by side and compare them.

II. NUMERICAL METHOD

The method used to solve numerically the Schrödinger equation relies on separating the wave function into its real and imaginary parts, as

$$\psi(x, t) = \mathcal{R}(x, t) + i\mathcal{I}(x, t), \quad (27)$$

and then use Runge Kutta's second order method to solve the coupled system of equations. Using the separation proposed in Eq. (27) and plugging this back in Eq. (4) yields a system of

partial differential equations for the real and imaginary parts, just as

$$\frac{\partial}{\partial t} \mathcal{R}(x, t) = -\frac{1}{2} \frac{\partial^2}{\partial x^2} \mathcal{I}(x, t) + V(x)\mathcal{I}(x, t), \quad (28a)$$

$$\frac{\partial}{\partial t} \mathcal{I}(x, t) = +\frac{1}{2} \frac{\partial^2}{\partial x^2} \mathcal{R}(x, t) + V(x)\mathcal{R}(x, t). \quad (28b)$$

As said before, these equations are coupled, so solving for one involves the other. As any numerical approach to differential equations of this type, we will discretize space and time, making those partials become tiny deltas and use our numerical method, which is a second-order Runge-Kutta.

I. Second order Runge Kutta

Suppose we have N coupled differential equations

$$\dot{x}_1 = f_1(x_1, \dots, x_N), \quad (29a)$$

$$\dot{x}_2 = f_2(x_1, \dots, x_N), \quad (29b)$$

⋮

$$\dot{x}_n = f_N(x_1, \dots, x_N). \quad (29c)$$

The procedure to solve these is to define first a set of k_1 's, one for each one of the N equations, defined as [11]

$$k_1^j = f_j(x_1, \dots, x_N)\Delta t, \quad (30)$$

where $1 \leq j \leq N$ and Δt is the discretized time. This k_1 is basically the displacement of the function $x_j(t)$ when a given interval Δt passes. Then, we define “half step” values, given by

$$x_j\left(t + \frac{\Delta t}{2}\right) = x_j + \frac{k_1^j}{2}, \quad (31)$$

and finally, we calculate the k_2 's,

$$k_2^j = f_j\left[x_1\left(t + \frac{\Delta t}{2}\right), \dots, x_N\left(t + \frac{\Delta t}{2}\right)\right]\Delta t. \quad (32)$$

The next time step is then given by

$$x_j(t + \Delta t) = x_j(t) + k_2^j. \quad (33)$$

Now we need to apply the described procedure to the wave function. The N coupled differential equations shown at Eqs. (29) will be, in the context of Schrödinger's equation, Eqs. (28).

Here, the values of $k_{1,2}^j$ will be denoted by $k_{1,2}^{\mathcal{R}}$ and $k_{1,2}^{\mathcal{I}}$, while the half-step values will be $\mathcal{R}_{1/2}$ and $\mathcal{I}_{1/2}$. Also, for computational purposes, we need to define indices in order to organize space and time, so it is of good practice to define

$$\begin{aligned} t &\rightarrow i, \\ t + \Delta t &\rightarrow i + 1, \\ x &\rightarrow n, \\ x + \Delta t &\rightarrow n + 1. \end{aligned}$$

Now that notation is established, the Runge-Kutta on second order procedure will start by calculating the k_1 's and half-steps:

$$\begin{aligned} k_1^R(i) &= -r [\mathcal{I}(i+1, n) - 2\mathcal{I}(i, n) + \mathcal{I}(i-1, n)] + V(i)\mathcal{I}(i, n)\Delta t, \\ k_1^T(i) &= +r [\mathcal{R}(i+1, n) - 2\mathcal{R}(i, n) + \mathcal{R}(i-1, n)] + V(i)\mathcal{R}(i, n)\Delta t, \\ \mathcal{R}_{1/2}(i) &= \mathcal{R}(i, n) + k_1^R(i)/2, \\ \mathcal{I}_{1/2}(i) &= \mathcal{I}(i, n) + k_1^T(i)/2. \end{aligned}$$

Then, the procedure continues calculating the k_2 's and the time evolution:

$$\begin{aligned} k_2^R(i) &= -r [\mathcal{I}_{1/2}(i+1) - 2\mathcal{I}_{1/2}(i) + \mathcal{I}_{1/2}(i-1)] + V(i)\mathcal{I}_{1/2}(i)\Delta t, \\ k_2^T(i) &= +r [\mathcal{R}_{1/2}(i+1) - 2\mathcal{R}_{1/2}(i) + \mathcal{R}_{1/2}(i-1)] + V(i)\mathcal{R}_{1/2}(i)\Delta t, \\ \mathcal{R}(i, n+1) &= \mathcal{R}(i, n) + k_2^R(i), \\ \mathcal{I}(i, n+1) &= \mathcal{I}(i, n) + k_2^T(i). \end{aligned}$$

The parameter r in front of the k 's appears naturally during the calculations, and it is given by

$$r = \frac{\Delta t}{2\Delta x^2}. \quad (34)$$

In practice, we use a pre-defined value of r to calculate Δx by means of isolating Δx on the above equation.

Besides the wave function, the program returns the energy associated with the system, which is

$$\langle \hat{H} \rangle = \frac{\int_{-\infty}^{+\infty} \psi^*(x, t)\hat{H}\psi(x, t)}{\int_{-\infty}^{+\infty} |\psi(x, t)|^2 dx}. \quad (35)$$

If we use the separation suggested in Eq. (27), we see that the Hamiltonian acts separately on the real and imaginary parts, as in

$$\hat{H}\psi(x, t) = \hat{H}\mathcal{R}(x, t) + i\hat{H}\mathcal{I}(x, t). \quad (36)$$

These terms, translated into our formalism presented so far, yield

$$\begin{aligned} \hat{H}\mathcal{R}(i, n) &= -\frac{1}{2} \frac{\mathcal{R}(i+1, n) - 2\mathcal{R}(i, n) + \mathcal{R}(i-1, n)}{\Delta x^2} + V(i)\mathcal{R}(i, n) \\ \hat{H}\mathcal{I}(i, n) &= -\frac{1}{2} \frac{\mathcal{I}(i+1, n) - 2\mathcal{I}(i, n) + \mathcal{I}(i-1, n)}{\Delta x^2} + V(i)\mathcal{I}(i, n) \end{aligned}$$

Thus, the energy, in its discretized version, is given by

$$E = \frac{\sum_i \psi^*(i, n)\hat{H}\psi(i, n)\Delta x}{\sum_i |\psi(i, n)|^2 \Delta x}. \quad (37)$$

II. User manual

The code is pretty straightforward, and Table 1 summarizes the parameters necessary for the function to run.

Parameter	Brief description
tf	Total time of simulation
dt	Time step of simulation
r	Parameter r discussed above
L	Spatial region considered
omega	Frequency of oscillation
n	Mode of oscillation
k0	Initial momentum

Table 1: Input parameters of Second Order Runge Kutta algorithm.

Notice that there is no dx as an input parameter, since it is defined based on the dt and r parameters. The outputs of the function are listed in Table 2.

Parameter	Brief description
Psi	Wave function
N	Normalization at each time
E	Energy at each time

Table 2: Output of the function.

The normalization was calculated using a pre-defined function of Numpy library, but other methods of integration as 1/3-Simpson method [11] should also work.

A quick note on the algorithm itself: at first it was written as three loops: one for the time indices i , then two separated loops for the space indices n , the first for calculating the k_1 's and the half steps, and the second to calculate the k_2 's. This would be computationally expensive, and with a help from Rodrigo Da Motta, I was able to eliminate both of the n -related loops. The resulting code is somewhat more cumbersome, but much more efficient.

III. RESULTS AND ANALYSIS

The main focus of the following analysis will be on observables and their expected values, as well as on the PDFs associated with the wave functions. However, it could be misleading to look at the PDF associated to the harmonic oscillator eigen-states and see a time-independent function. It raises the question: where are the oscillations of the so-called harmonic oscillator? Well, it is on the wave function itself. Refer to the supplementary material provided on [Notion](#) to see an animation showing that both real and imaginary parts of the wave function are indeed oscillatory, where the first excited state was used as example.

I. First vibration modes

The first few modes of vibration PDFs are shown in Fig. 2, where they are displayed according to their energy level. Although this

representation is nice, one needs to be careful with it, since the probability distribution of mode ψ_n has zero amplitude at E_n in the y-axis. This remark being said, the first thing to notice is that the probability of finding the particle outside the potential is not zero, which is strikingly different from the classical oscillator. Another property, a heritage from the Hermite polynomials in Eq. (13), is that modes of vibration with n odd result in a zero chance of finding the particle at $x = 0$.

As the energies get bigger, we see more bumps in the probability distribution; however these bumps have their amplitudes getting smaller in size. This shrinking feature is expected, since all the PDFs need to be normalized. Also, something that suggests a resemblance with the classical oscillator is the probability at the edges of the potential being bigger than the ones more internal for $n \geq 1$. This feature relates to the PDF for the classical oscillator shown in Fig. 1.

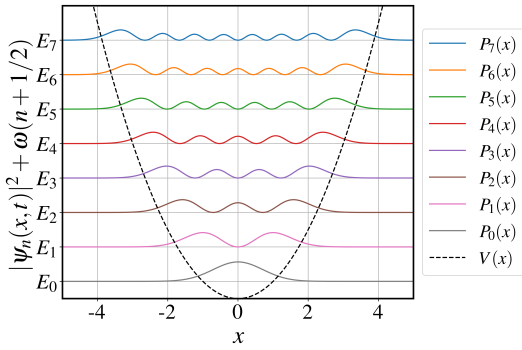


Figure 2: The first seven probability density functions of the harmonic oscillator, according to their energies. Each curve shows the PDF for one mode of vibration, and the dashed curve shows the harmonic potential. Parameters used: $t_f = 0.05$, $dt = 10^{-5}$, $r = 0.075$, $L = 5$, $\omega = 1$.

Another good visualization can be seen in Fig. 3. The information is basically the same, but now we have a good look of the effect from the harmonic potential: the chance of finding the oscillator is biggest at the vicinity where its energy crosses the potential, as suggested in the paragraph above.

It is worth noticing that, as expected from previous development, the modes of vibration are stationary: their PDFs are time-independent, so what we see in Figs. 2 and 3 are the whole story; there is no change in it as time passes.

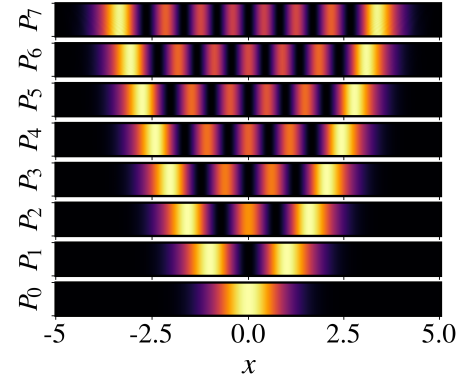


Figure 3: Heatmap of the first few modes. The information here is similar to the one shown in Fig. 2: as the energy gets bigger, the oscillator wiggles more and is more evenly distributed along the potential. Same parameters were used.

Another aspect that can be considered is the relation between the classical and harmonic oscillator. In Fig. 4 we can see the PDFs of the quantum oscillator for various vibration modes, along with its classical associated oscillator with same energy. We see that for smaller energies the PDF's have a big discrepancy, but as n gets bigger, there is a clear trend: they start to coincide.

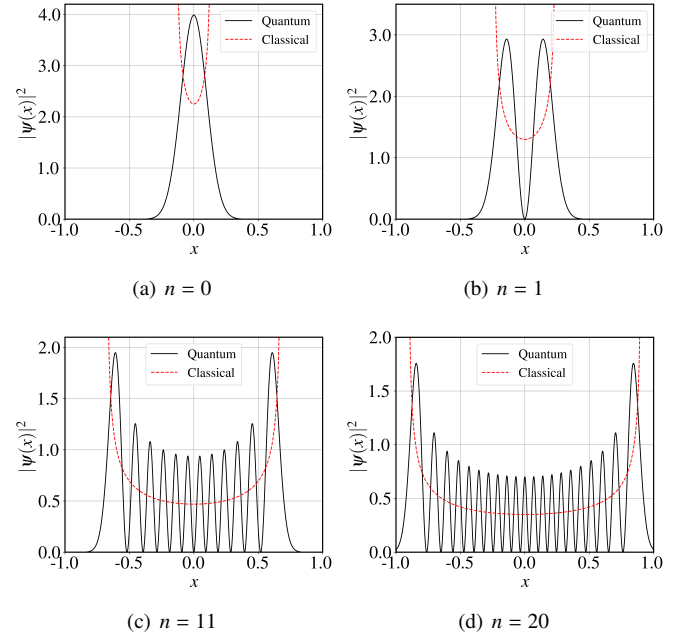
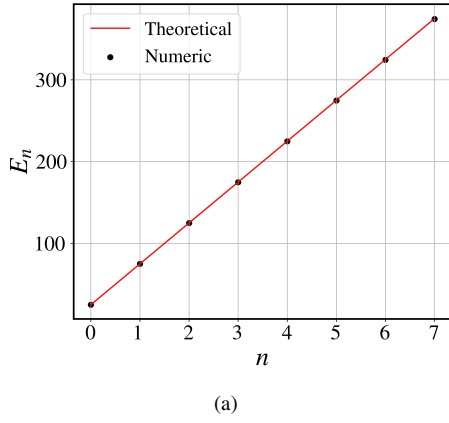


Figure 4: Comparison between the probability density function of the quantum and the classical harmonic oscillator with energy E_n . Parameters used: (a) $dt = 10^{-5}$, $r = 0.075$, $\omega = 50$; (b) same as (a); (c) $dt = 10^{-6}$; (d) $dt = 10^{-6}$.

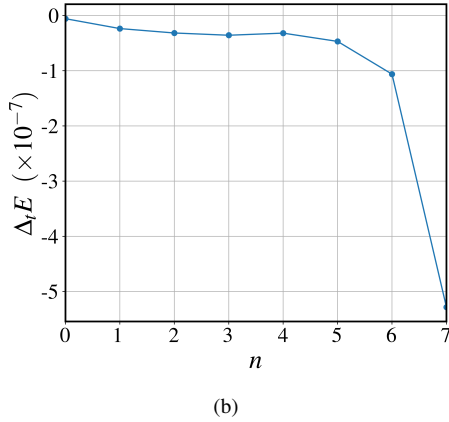
The correspondence principle states that at n infinitely large,

the quantum and classical distributions must coincide. The reason is that for large energies, the quantum version oscillates so rapidly that only the mean value of its position is detected, and it eventually coincides with P_{cl} [10, 3].

The energies of the oscillator are shown in Fig. 5(a). We can see good agreement with the theoretical prediction from Eq. (15). Since in this study the units are such that $m = \hbar = 1$, the dimensions of energy are given in terms of frequency. These energies were measured at the beginning of the simulation, and they must maintain constant during the whole course of it, since this is a conservative system. Indeed, the energies remain very consistent throughout the simulation for the given time, as can be seen in Fig. 5(b), that displays the difference in energy at time $t = 0$ and $t = t_f$ for the first eight modes of oscillation. Although the difference is small for the modes considered, we can clearly see a trend of growth as n gets bigger.



(a)



(b)

Figure 5: (a) The first few energy modes for the quantum harmonic oscillator at initial times. The black dots are the numerically simulated ones, while the red line represents the theoretical prediction. (b) Difference between the energies calculated at $t = 0$ and at $t = t_f$, for the first few modes of oscillation. Parameters used: $t_f = 0.05$, $dt = 10^{-5}$, $r = 0.075$, $L = 1$, $\omega = 50$.

II. Time step and r parameter

The reason for the time step of curves shown in Figs. 4(c) and 4(d) being smaller is a matter of visualization, since it provides a smoother curve. Something found during the simulations is that for bigger energies, i.e. bigger n values, not only the smoothness of the curves, but also the normalization and the energies of the PDFs are jeopardized, as can be seen in Fig. 6, where is displayed a relation between the initial normalization of the PDF and the mode of oscillation. A feature of this error effect was noticed for the initial and final energies in Fig. 5(b), since it affects the simulation during all of its course.

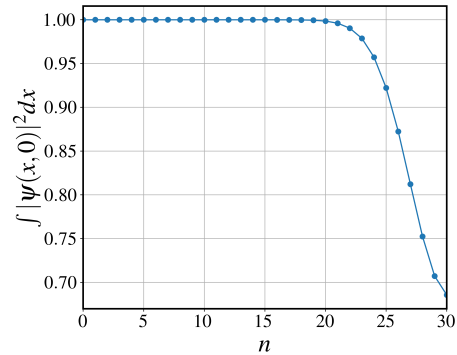


Figure 6: Normalization of the initial state as a function of n . We can see that the normalization begins to fail rapidly shortly after $n = 20$. Parameters used: $t_f = 0.05$, $dt = 10^{-5}$, $r = 0.075$, $L = 1$, $\omega = 50$.

It was also noticed that for bigger times the normalization completely diverges. This effect is related to the accumulated error in the second order Runge-Kutta method, and seems to be due to the frequency of oscillations of the wave function that grow rapidly as we increase the values of n . Thus, the time step of the simulation needs to be further shortened in order to capture the rapid dynamics of the oscillator at higher energies.

III. Uncertainty relation

In Fig. 7 we can see the uncertainty relation for the seven first modes of vibration. We can see that it increases linearly with n as depicted in Eq. (20).

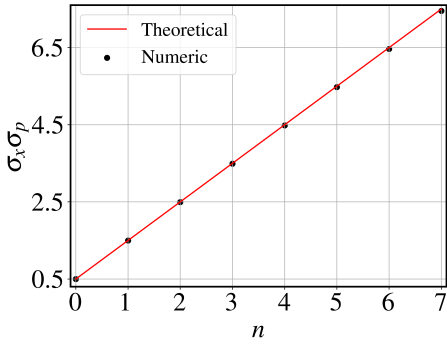


Figure 7: Uncertainty relation for various modes of oscillation. The black dots represent the numeric simulations, while the red line represents the theoretical prediction, according to Eq.(20).

As preconceived earlier, the lower bound of the uncertainty principle is obtained with the ground-state of the harmonic oscillator, and this result is independent of the frequency of oscillation. The numeric result serves as a validation for the previous theoretical prediction.

IV. Addition of a spatial phase

An interesting aspect to explore is if we plug in our initial state some kind of *spatial phase*, so instead of ϕ_0 , we use

$$\psi(x, 0) = \phi_0(x) e^{ik_0 x} \quad (38)$$

which leads a time evolution

$$\psi(x, t) = \phi_0(x) e^{ik_0 x} e^{-iE_0 t} \quad (39)$$

To check the effect of introducing this imaginary exponential term, we can calculate the expected values of some important operators. Position and momentum's initial expected values will be

$$\langle \hat{x} \rangle_0 = \int_{-\infty}^{+\infty} \phi_0 e^{-ik_0 x} x \phi_0 e^{ik_0 x} dx = 0, \quad (40a)$$

$$\langle \hat{p} \rangle_0 = -i \int_{-\infty}^{+\infty} \phi_0 e^{-ik_0 x} \frac{\partial}{\partial x} (\phi_0 e^{ik_0 x}) dx = k_0. \quad (40b)$$

Thus, the addition of a spatial phase does not change the initial position expected value, although it changes momentum's: it is as if we gave a k_0 initial boost to the system. Increasing system's momentum must increase its overall energy, which is true if we calculate $\langle H \rangle$ over the state given in Eq. (38):

$$\langle H \rangle = \frac{1}{2} (\omega + k_0^2) = E_0 + \frac{k_0^2}{2}. \quad (41)$$

As a validation of our prediction in Eq. (41) it is possible to examine the effect of k_0 in the displacement of the energies.

Figs. 8 and 9 show two different scenarios: the former is the variation of the ground state energy with k_0 , while the later is a $E_n \times n$ curve for various values of k_0 .

Fig. 8 confirms Eq. (41): the ground state energy changes quadratically with k_0 . This is indeed expected, since the initial boost in momentum should affect the ground state energy.

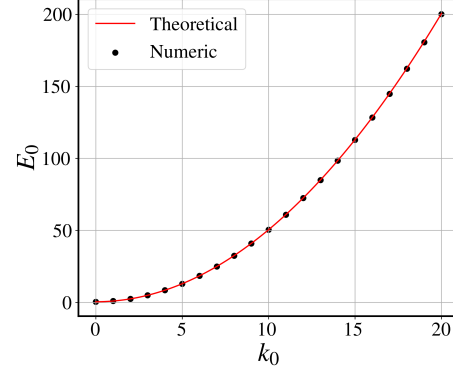


Figure 8: Plot of $E_0 \times k_0$, validating the prediction that the ground state energy is proportional to k_0 quadratically. Parameters used: $t_f = 0.05$, $dt = 10^{-5}$, $r = 0.075$, $L = 5$, $\omega = 1$, $n = 0$ and varying k_0 from 0 to 20.

Fig. 9 shows that the excited states still change linearly with n —which is pretty much the same behavior depicted by Fig. 5(a)—but they all suffer a shift of $k_0^2/2$. This strongly suggests that we generalize our Eq. (41) to

$$E_n^{k_0} = E_n + \frac{k_0^2}{2}, \quad (42)$$

where E_n is the energy as if $k_0 = 0$.

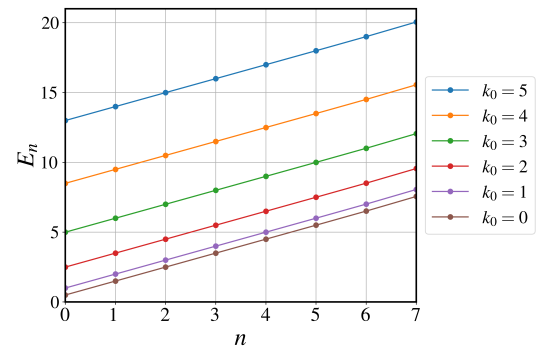


Figure 9: Plot of $E_n \times n$ for different values of k_0 . It shows a displacement between the curves of exactly $k_0^2/2$ units of energy, suggesting that Eq. (41) is generalized to Eq. (42). Parameters used: $t_f = 0.05$, $dt = 10^{-5}$, $r = 0.075$, $L = 5$, $\omega = 1$.

Although the expected value for the position operator \hat{x} is not affected at all by the initial boost k_0 , there is some interest-

ing dynamics happening that is related to $\langle \hat{p} \rangle$ being non-trivial. Referencing Ehrenfest's theorem as announced in Eqs. (25), it is possible to see that since the time evolution of both of the observables are mutually dependent, even $\langle \hat{x} \rangle$ will wiggle due to $\langle \hat{p} \rangle_0 \neq 0$. This behavior is shown in Fig. 10, which displays $\langle \hat{x} \rangle_t$ and $\langle \hat{p} \rangle_t / \omega$ as functions of time.

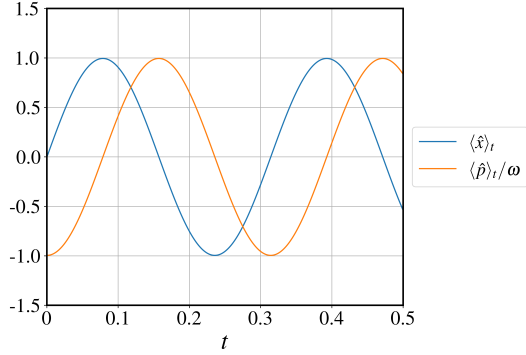


Figure 10: Expectation values of \hat{x} and \hat{p} , as foreseen by Ehrenfest's theorem. We can see that, as the classical harmonic oscillator, there is a phase factor between them. Parameters used: $t_f = 0.5$, $dt = 10^{-5}$, $r = 0.075$, $L = 1$, $\omega = k_0 = 20$, $n = 0$.

Since $\langle \hat{x} \rangle_0 = 0$, the two curves are basically a sine and a cosine with amplitude given by $\langle \hat{p} \rangle / \omega$ and $\omega \langle \hat{p} \rangle$ respectively, which explains the difference in phase that must be very close to $\pi/2$. This is the reason why the evolution of the linear momentum is divided by ω : these do not have the same magnitude and would be difficult to see them simultaneously without any kind of normalization.

Since the expected value of the positions is changing with time, as a consequence the peak of the Gaussian wave packet oscillates. An animation of this motion is provided in the supplementary material at [Notion](#). We can see that the resulting PDF is at the same time shape-preserving, since it remains a Gaussian during the whole time, but it keeps oscillating as time passes. As a matter of definition, we can say that this state is not stationary, since its momentum and position are time-dependent.

V. Linear combination of eigen-states

As exposed earlier, the set $\{\phi_n\}$ of all eigen-states of the harmonic oscillator Hamiltonian constitute a complete set and can be used as a base for expansion of arbitrary initial states. A little demonstration of this feature was done, using an initial state

$$\varphi(x, 0) = \frac{1}{\sqrt{3}} \sum_{n=0}^2 \phi_n. \quad (43)$$

Fig. 11 shows the probability distribution associated with the above initial state, at three different times. Clearly the PDF

changes its shape over time, showing that it is no longer time independent. For further reference, check [Notion](#) for an animation of the PDF distribution.

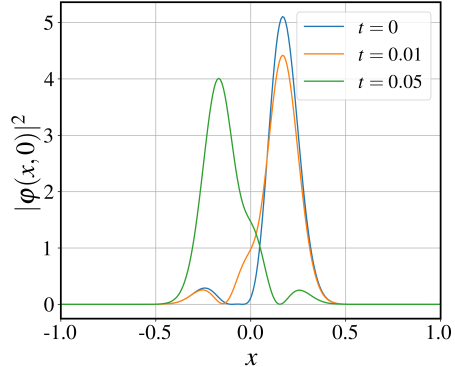


Figure 11: PDF for an initial state given by the linear combination of the first three modes of oscillation, at three different times, showing that the probability distribution is no longer time-independent. Parameters used: $t_f = 0.05$, $dt = 10^{-5}$, $r = 0.075$, $L = 1$, $\omega = 50$, $k_0 = 0$.

As for the normalization of this state, the difference between the initial and final times is $\sim 10^{-6}$, which shows a good normalization overall. This good behavior probably is broken when more eigen-states are included in the linear combination, as well as more energetic ones.

IV. CONCLUSION

Albeit second order Runge-Kutta method for solving the Schrödinger equation shows good agreement with the theoretical predictions developed in the Introduction section, it is strongly recommended to be cautious when setting the duration of the simulation, as well as the discretization of time and the definition of parameter r . Big discrepancies arises at times large enough, i.e. times bigger than one period of oscillation.

There are resemblances as well as deep discrepancies between the classical and quantum oscillators, as were pointed out by the investigations of the energy modes of vibration and the probability distributions in both regimes—quantum and classical. For instance, the classically prohibited region of oscillation has non-zero probability amplitude in the quantum case, meaning that it is possible to find the oscillating particle in these areas.

The addition of a spatial phase creates interesting dynamical scenarios to explore, where the expected values of position and momentum vary with time; something that otherwise is not possible for the harmonic oscillator's eigen-states, that are stationary.

Further investigation of an initial state as LC of eigen-states show good normalization properties, although it can be jeopardized for more (and more energetic) terms. These PDFs are

time-dependent and can be animated.

As suggestions for improvements of this study I point out a further analysis of the simulation parameters and its relation with Runge-Kutta accumulated error, especially for long periods of time; as well as the simulation of a linear combination of eigen-states together with a spatial phase e^{ik_0x} and its effect on the observables and the PDF associated with the resulting wave function.

REFERENCES

- [1] R. Eisberg and R. Resnick. *Quantum Physics of Atoms, Molecules, Solids, Nuclei and Particles*. John Wiley & Sons, 2nd edition, 1985.
- [2] G. T. Landi. Quantum information and quantum noise. http://wwwfmt.if.usp.br/~gtlandi/courses/lecture-notes_v2-18.pdf, 2019.
- [3] D. J. Griffiths and D. F. Schroeter. *Introduction to quantum mechanics*. Cambridge university press, 3rd edition, 2018.
- [4] C. C. Tannoudji, B. Diu, and F. Laloe. *Quantum Mechanics*, volume 1. Wiley-VCH, 2nd edition, 2020.
- [5] J. J. Sakurai and J. Napolitano. *Modern Quantum Mechanics*. Pearson, 2nd edition, 2011.
- [6] P. A. M. Dirac. *Principles of Quantum Mechanics*. Oxford University Press, 3rd edition, 1948.
- [7] S. Hawking. *The Universe in a Nutshell*. Bantam, 2001.
- [8] R. L. Liboff. *Introductory Quantum Mechanics*. Addison-Wesley Publishing Company, 1980.
- [9] E. Merzbacher. *Quantum Mechanics*. John Wiley & Sons, Inc., 3rd edition, 1998.
- [10] R. Shankar. *Principles of Quantum Mechanics*. Plenum Press, 2nd edition, 1994.
- [11] Eduardo Colli and Claudio H. Asano. Cálculo numérico: Fundamentos e aplicações, Dezembro 2009.